

Optimized Methods for the Production of High-Purity ^{203}Pb Using Electroplated Thallium Targets

Shefali Saini¹, Jennifer L. Bartels¹, Jean-Pierre K. Appiah¹, Jason H. Rider¹, Nicholas Baumhover², Michael K. Schultz², and Suzanne E. Lapi¹

¹Department of Radiology, University of Alabama at Birmingham, Birmingham, Alabama; and ²Perspective Therapeutics, Inc., Coralville, Iowa

^{203}Pb is a surrogate imaging match for ^{212}Pb . This elementally matched pair is emerging as a suitable pair for imaging and targeted radionuclide therapy in cancer care. Because of the half-life (51.9 h) and low-energy γ -rays emitted, ^{203}Pb is suitable for the development of diagnostic radiopharmaceuticals. The aim of this work was to optimize the production and separation of high-specific-activity ^{203}Pb using electroplated thallium targets. We further investigated the radiochemistry optimization using a suitable chelator, tetraazacyclododecane-1,4,7-triacetic acid (DO3A), and targeting vector, VMT- α -NET (lead-specific chelator conjugated to tyr3-octreotide via a polyethylene glycol linker). **Methods:** Targets were prepared by electroplating of natural or enriched (^{205}Tl) thallium metal. Scanning electron microscopy was performed to determine the structure and elemental composition of electroplated targets. Targets were irradiated with 24-MeV protons with varying current and beam time to investigate target durability. ^{203}Pb was purified from the thallium target material using an extraction resin (lead resin) column followed by a second column using a weak cation-exchange resin to elute the lead isotope as $[\text{}^{203}\text{Pb}]\text{PbCl}_2$. Inductively coupled plasma mass spectrometry studies were used to further characterize the separation for trace metal contaminants. Radiolabeling efficiency was also investigated for DO3A chelator and VMT- α -NET (a peptide-based targeting conjugate). **Results:** Electroplated targets were prepared at a high plating density of 76–114 mg/cm² using a plating time of 5 h. A reproducible separation method was established with a final elution in HCl (400 μL , 1 M) suitable for radiolabeling. Greater than 90% recovery yields were achieved, with an average specific activity of 37.7 ± 5.4 GBq/ μmol (1.1 ± 0.1 Ci/ μmol). **Conclusion:** An efficient electroplating method was developed to prepare thallium targets suitable for cyclotron irradiation. A simple and fast separation method was developed for routine ^{203}Pb production with high recovery yields and purity.

Key Words: lead-203; thallium-205; electroplating; DO3A; radiolabeling

J Nucl Med 2023; 00:1–7

DOI: 10.2967/jnumed.123.265976

Radiopharmaceuticals can be used for diagnostic or therapeutic applications based on the incorporated radionuclide. The term *theranostic* is a portmanteau word for *therapy* and *diagnostic*. In theranostics, an imaging surrogate is used to guide delivery of a personalized dosage for a disease condition (1,2). In nuclear medicine, theranostic radiopharmaceuticals use a common precursor to

diagnose and treat the disease condition using radionuclides with similar or identical chemistry but decay properties that are suitable for imaging and therapy (3). In this context, ^{203}Pb and ^{212}Pb represent an elementally identical radioisotope pair that is particularly well suited for the development of theranostics.

Food and Drug Administration approved agents such as NET-SPOT ($[\text{}^{68}\text{Ga}]\text{Ga-DOTATATE}$; Advanced Accelerator Applications) and LUTATHERA ($[\text{}^{177}\text{Lu}]\text{Lu-DOTATATE}$; Novartis) are routinely used in clinical settings for the diagnosis and therapy of somatostatin receptor positive neuroendocrine tumors (4,5). However, despite the potential of these theranostic agents, different radionuclides for imaging and therapy may often require different methods for chemistry optimization and different chelators. In addition, the in vivo biodistribution profiles of these radiopharmaceuticals labeled with ^{68}Ga or ^{177}Lu may be different (6,7). Therefore, to better match the diagnostic and therapeutic counterparts, elementally matched isotope pairs are highly desired. Elementally matched radiopharmaceuticals use the same radioactive element with isotopes that have decay properties making them suitable for diagnostic imaging (β^+ / γ -emitting) and therapeutic (α/β^- emitting) applications. In this way, the in vivo biodistribution is identical and the imaging surrogate can be used to understand and predict the pharmacokinetics of the therapeutic. In addition, the use of an elementally matched isotope pair for theranostics adds confidence to dosimetry, thereby providing potentially more accurate treatment planning. Table 1 provides a list of elementally matched isotopes for theranostic matched pairs.

^{203}Pb and ^{212}Pb are an emerging, elementally matched pair of high interest. ^{203}Pb decays to stable ^{203}Tl by electron capture with the emission of a low-energy γ -photon (279 keV, 81%) and no radioactive daughter, making it suitable for SPECT imaging applications (8). ^{212}Pb is a daughter of ^{224}Ra and decays by emitting 2 β^- and one α particle, making it suitable for therapeutic applications (9–11). ^{212}Pb is typically available from a $^{224}\text{Ra}/^{212}\text{Pb}$ generator, but commercial-scale manufacturing is feasible because of relatively straightforward chemistry for purification.

The present study investigated the production of ^{203}Pb via proton irradiation of thallium targets ($^{205}\text{Tl}(p,3n)^{203}\text{Pb}$) and development of a robust separation method to obtain a final product of high specific activity. A simple 2-column separation method was developed that requires small elution volumes with a separation time of less than 2 h. The final product was eluted in HCl (400 μL , 1 M), making it feasible for radiolabeling and shipping to other facilities. Further evaluation for radiolabeling was performed with a DO3A chelator to develop a standard operating procedure for apparent molar activity (AMA) analysis. Elemental analysis was determined using inductively coupled plasma mass spectrometry (ICP-MS) to analyze the impurities in the final product.

Received May 4, 2023; revision accepted Jul. 17, 2023.

For correspondence or reprints, contact Suzanne E. Lapi (lapi@uab.edu).

Published online Aug. 31, 2023.

COPYRIGHT © 2023 by the Society of Nuclear Medicine and Molecular Imaging.

TABLE 1
Characteristic Properties of Elementally Matched Theranostic Isotope Pairs

Diagnostic				Therapeutic				Reference
Radionuclide	Half-life	Decay	Energy* (keV)	Radionuclide	Half-life	Decay	Energy* (keV)	
²⁰³ Pb	51.8 h	EC (100%)	279 (81%)	²¹² Pb	10.6 h	β ⁻ (100%)	β ⁻ : 40.9 (5%), 93.3 (81.5%), 171.4 (13.7%), γ: 238 (46.3%)	(8,22)
⁶⁴ Cu	12.7 h	β ⁺ (17.8%), EC (43.8%)	511 (35%), 1,345 (0.5%)	⁶⁷ Cu	61.9 h	β ⁻ (100%)	395 (45%), 484 (35%), 577 (20%)	(23,24)
⁸⁶ Y	14.7 h	β ⁺ (31.9%), EC (68.1%)	443 (16.9%), 628 (32.6%)	⁹⁰ Y	64 h	β ⁻ (100%)	932.4 (99.9%)	(25,26)
¹²⁴ I	4.2 d	β ⁺	603 (61%), 1,691 (11%)	¹³¹ I	8 d	β ⁻ (100%)	284 (6.14%), 365 (81.7%), 637 (7.17%)	(27,28)
¹⁵² Tb	17.5 h	β ⁺ + EC (100%)	344 (63.5%)	¹⁴⁹ Tb	4.1 h	α (17.7%)	α: 3 967	(29,30)
¹⁴⁹ Tb	4.1 h	EC (82.3%)	165 (26.7%), 352 (29.8%), 388.6 (18.6%)	¹⁶¹ Tb	6.9 d	β ⁻ (100%)	137.7 (25.7%), 157.4 (65%)	
¹⁵⁵ Tb	5.3 d	EC (100%)	86.5 (32%), 105.3 (25%), 180 (7.5%)					
⁴³ Sc	3.9 h	β ⁺ (98%),	373 (22.5%)	⁴⁷ Sc	3.3 d	β ⁻ (100%)	159.4 (68%)	(31–35)
^{44g} Sc	3.9 h	β ⁺ (94%)	1,157 (100%)					

*Intensity.

EC = electron capture.

MATERIALS AND METHODS

All reagents were purchased from Sigma Aldrich unless otherwise noted. Additional details are provided in the supplemental materials (supplemental materials are available at <http://jnm.snmjournals.org>).

Thallium Target Preparation by Electroplating

An electroplating bath was prepared following the procedure from Suparman with some modifications (12). Briefly, the electroplating bath was prepared by mixing 250 mg of [^{nat}Tl]Tl₂O₃ or [²⁰⁵Tl]Tl₂O₃, hydrazine hydrate (300 μL), NaOH (1 g), and ethylenediaminetetraacetic acid (1.5 g) in 10 mL of water. Copper (1.5-mm thickness) or gold (1-mm thickness) backings of 25-mm diameter were used as the cathodes. An electroplating station (Fig. 1) was designed and manufactured to help optimize uniform target mass deposition on a copper or gold coin. The details of the procedure are provided in the supplemental materials.

Target Irradiation and Purification of ²⁰³Pb

All target irradiations were performed on an Advanced Cyclotron Systems TR24 cyclotron. Using an Advanced Cyclotron Systems 90° solid target holder (13), electroplated target disks of ²⁰⁵Tl were manually loaded in the target holder and irradiated at 24 MeV with varying currents from 5 to 40 μA and durations of 15 min to 3 h. The optimal beam profile and transmission were determined through maximization of the ion source injection system and the beamline vertical and horizontal focusing quadrupole magnet system settings on the cyclotron. With an effective beam energy of 24 MeV, the best transmission ratio was 93% with a 10%–15% beam spill on target collimators (top/bottom and left/right). A higher beam spill was chosen to help with cooling, provide better beam spread, and avoid a pinpoint beam spot

that leads to target failure. With a pneumatic release system, irradiated target disks were loaded into lead containers and transferred for further processing. Targets were left overnight to allow for decay of short-lived isotopes, including ²⁰¹Pb (half-life, 9.3 h) and ^{204m}Pb (half-life, 67.2 min).

For separation of ²⁰³Pb from the thallium target material, irradiated targets were dissolved in HNO₃ (5–7 mL, 2 M) with gentle heating to 90°C. The dissolved target was loaded onto a solid-phase extraction column (1 mL) containing an extraction resin (lead resin; Eichrom) (50 mg), which was preconditioned with water (10 mL) and HNO₃ (10 mL, 2 M). The solution was pushed through the column at 0.5–0.8 mL/min using a syringe or peristaltic pump. The resin was washed with additional HNO₃ (10 mL, 2 M) to allow maximum removal of thallium target material from the resin bed. ²⁰³Pb was eluted using sodium acetate (5 mL, 1 M, pH 5.5). This elution was loaded onto a second column containing 50 mg of weak cation-exchange resin previously preconditioned with water (5 mL) and NaOAc (5 mL, 1 M, pH 5.5). The resin was washed with HCl (1 mL, 0.01 M), and ²⁰³Pb was eluted as [²⁰³Pb]PbCl₂ using HCl (400 μL, 1 M). The fractions were analyzed with γ-ray spectroscopy. The separation scheme is shown in Figure 2.

ICP-MS

To investigate the trace metal impurities, ICP-MS analysis (Agilent 7700x) was performed for common contaminants including thallium, iron, copper, zinc, and stable lead in the final elution. Details of sample preparation are provided in the supplemental materials.

AMA Evaluation

AMA (GBq/μmol) was calculated by titration of [²⁰³Pb]PbCl₂ with DO3A chelator (Supplemental Fig. 1B). The ratio of radiolabeling

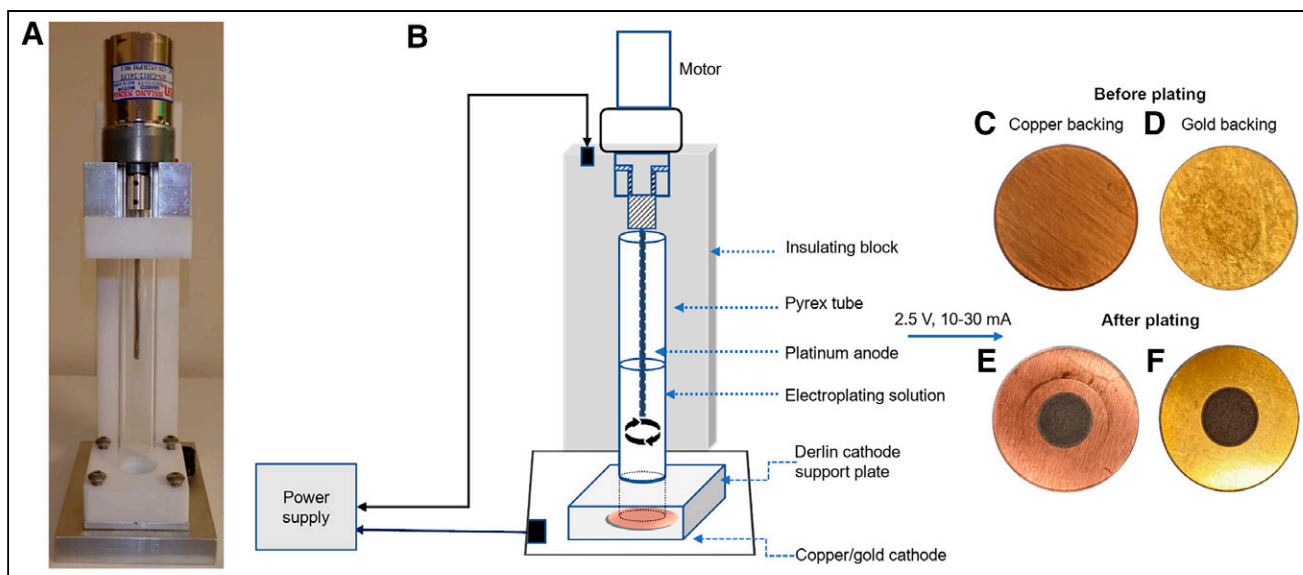


FIGURE 1. (A and B) Electroplating setup used for target preparation. (C–F) Copper and gold backings before (C and D) and after (E and F) electroplating.

yield (%) versus concentration of chelator ($\log[\text{DO3A}]$ [μmol]) was plotted using GraphPad Prism for the half-maximal effective concentration calculation. Results are reported as GBq (Ci)/ μmol . Complexation was analyzed using instant thin-layer chromatography silica gel (iTLC-SG) using 50 mM ethylenediaminetetraacetic acid as the mobile phase.

Radiolabeling

The VMT- α -NET targeting conjugate (Supplemental Fig. 1B) was used for radiolabeling studies (14). Stocks were prepared in NH_4OAc (0.5 M, pH 5). Radiolabeling was performed using mass amounts from 100 to 0.5 μg of the desired compound. Reactions were incubated for 20 min at 70°C. Instant thin-layer chromatography silica gel plates were used to confirm complexation using 50 mM ethylenediaminetetraacetic acid as the mobile phase. Results were analyzed using GraphPad Prism and reported as MBq (mCi)/mmol.

RESULTS

Electroplated Thallium Target Preparation

To produce ^{203}Pb , thallium metal (^{205}Tl) was used to prepare targets. Extreme toxicity, low melting point, and nonavailability

of thallium metal foils led us to explore an electroplating approach to target preparation (15,16). Electroplating conditions were optimized for electroplating periods extending from 1 to 5 h and solution pH ranging from 8 to 13. An approximately 14.5 ± 4 mg/h plating rate with a plating density of 76–114 mg/cm² was achieved on a regular basis ($n = 16$), and a pH of more than 12.5 was found to be most suitable for rapid deposition of thallium metal. The electroplating bath could be reused several times (~ 7 –8 reactions) with regular replenishing of target material, which eliminated the need to recycle the target material after every plating cycle. However, further investigation is required to develop a methodology for recycling the starting thallium metal. A schematic of the electroplating setup used for the plating process is shown in Figure 1. Targets were prepared on copper and gold backings.

To analyze the relationship between target density and plating time, targets were plated for 1 and 5 h. Scanning electron microscopy was performed on the electroplated targets to determine the structure and elemental composition of the target prepared. For thallium targets prepared on copper and gold backings, there were observable differences between the 1- and 5-h plating patterns in scanning electron microscopy analysis, indicating a nonuniform plating at 1 h whereas a uniform plating pattern was observed at the 5-h plating time point (Figs. 3A and 3B). However, gold backings showed uniform plating patterns at both the 1-h and the 5-h plating time points (Figs. 3D and 3E). Overall, $75\% \pm 5\%$ of the thallium in the electroplating solution was deposited after 5 h. In addition, the percentage deposition of thallium in the final plating was found to be independent of plating time. Both gold and copper backings were observed to have approximately $89.3\% \pm 1.6\%$ (by weight) thallium element deposited, with the remainder of the material composed of oxygen for both 1 h and 5 h as shown in the

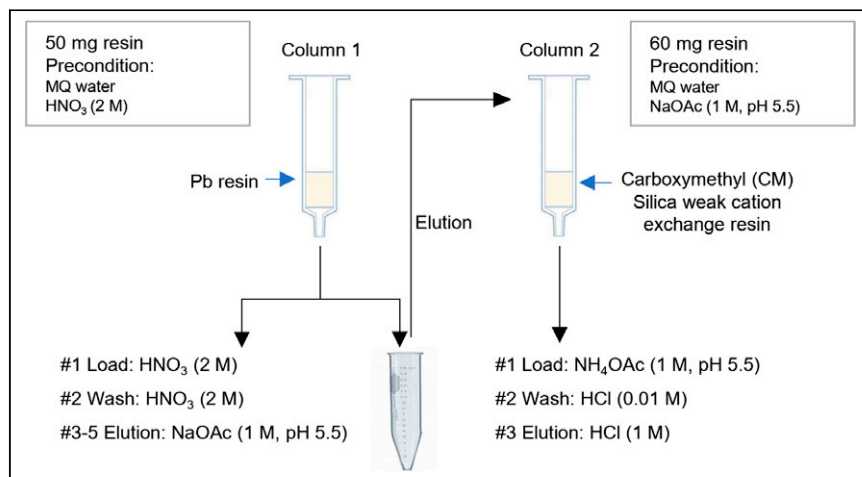


FIGURE 2. Separation scheme of ^{203}Pb purification from thallium target material. MQ = Milli-Q (Millipore Sigma).

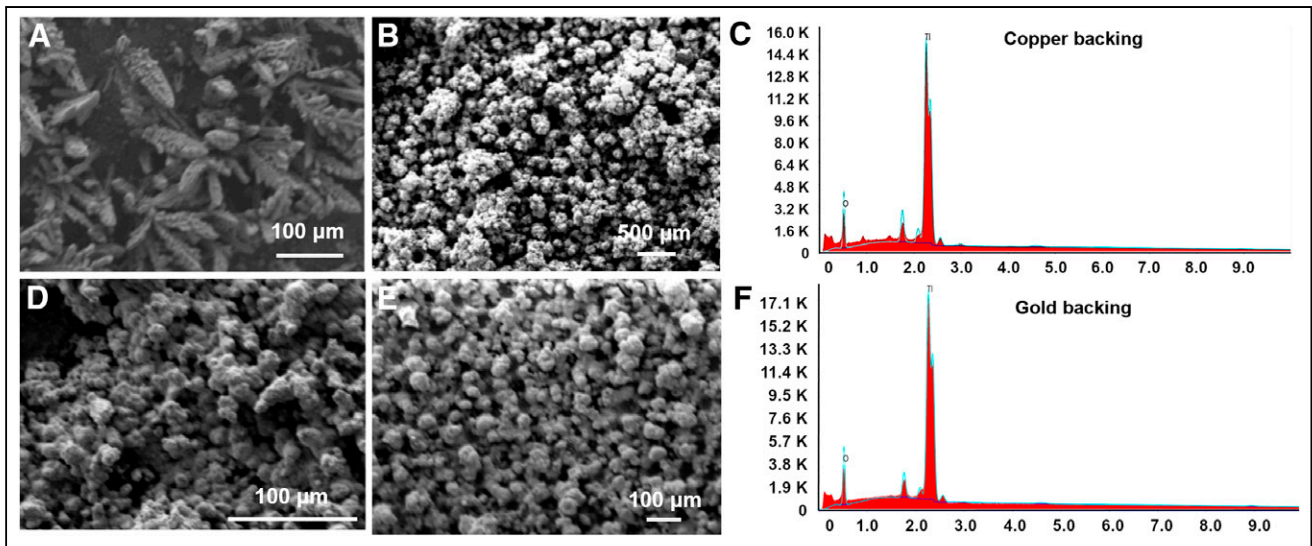


FIGURE 3. Representative scanning electron microscopy images of copper (top) and gold (bottom) backing. (A and B) Analysis at 1 h after plating. (D and E) Five-hour time point for copper and gold backing, respectively. (C and F) Energy-dispersive x-ray analysis spectra for both gold and copper backing, respectively.

energy-dispersive x-ray analysis spectra in Figures 3C and 3F. Since thallium has a very high propensity to oxidize (15), a significant amount of oxygen ($10.6\% \pm 1.6\%$) was also observed in scanning electron microscopy analysis. No other elemental peaks were found in the energy-dispersive x-ray analysis spectra. To achieve the production of the highest-purity ^{203}Pb possible, we explored the use of a 99.1% enriched ^{205}Tl target material, which contained trace levels of other contaminants such as silver, zinc, boron, sodium, and silicon as described in the material's certificate of analysis (Supplemental Table 1). The elemental analysis of the plated target material by scanning electron microscopy confirmed the presence of only thallium and oxygen, suggesting that high-purity ^{205}Tl targets are achievable if electroplating is used.

Target Irradiation and Purification of ^{203}Pb

The complete separation scheme of ^{203}Pb from thallium target material is as shown in Figure 4. We observed negligible ($<2\%$) lead isotopes in the eluate and nitric acid wash, whereas the lead isotopes were eluted in NaOAc buffer (5 mL, 1 M, pH 5.5) in the first column. During optimization of the separation procedures, we observed inconsistency in the chemical behavior of ^{203}Pb when stored in NaOAc for a longer period, which was most likely due to its hydrolyzation at this pH. In addition, to achieve more than 95% elution of ^{203}Pb , a large volume of NaOAc buffer (5–6 mL) was required. Therefore, concentration and purification of the elution from buffer to a more suitable labeling concentration was required. To address these challenges, a second column was used to further purify the ^{203}Pb . Final elution of ^{203}Pb separation from the enriched thallium target (^{205}Tl) was achieved in a small fraction of HCl ($\sim 400\ \mu\text{L}$, 1 M), with average recovery yields of $92.3\% \pm 3.5\%$ ($n = 3$). At the end of processing, $4,477 \pm 444\ \text{MBq}$ ($121 \pm 12\ \text{mCi}$) ^{203}Pb was obtained in the final elution (decay corrected to end of bombardment). The isotopic composition of the final elution product was found to be ^{203}Pb ($>99.5\%$) and ^{201}Pb ($<0.5\%$) as analyzed by γ -ray spectroscopy. The average production yields of $32.9 \pm 6.3\ \text{MBq}/\mu\text{A}\cdot\text{h}$ ($0.9 \pm 0.2\ \text{mCi}/\mu\text{A}\cdot\text{h}$) were achieved with a $98 \pm 16\ \text{mg}$ target.

Our separation method required about 1 h from column loading to elution from the second column, with a very small final volume ($<400\ \mu\text{L}$) and more than a 95% recovery yield.

ICP-MS

ICP-MS analysis was performed to further quantify the separation method and determine the presence of trace metal contamination. Results were compared for enriched ^{205}Tl targets for copper and gold backings as shown in Table 2. The method developed indicated a good separation, with only a small amount of thallium

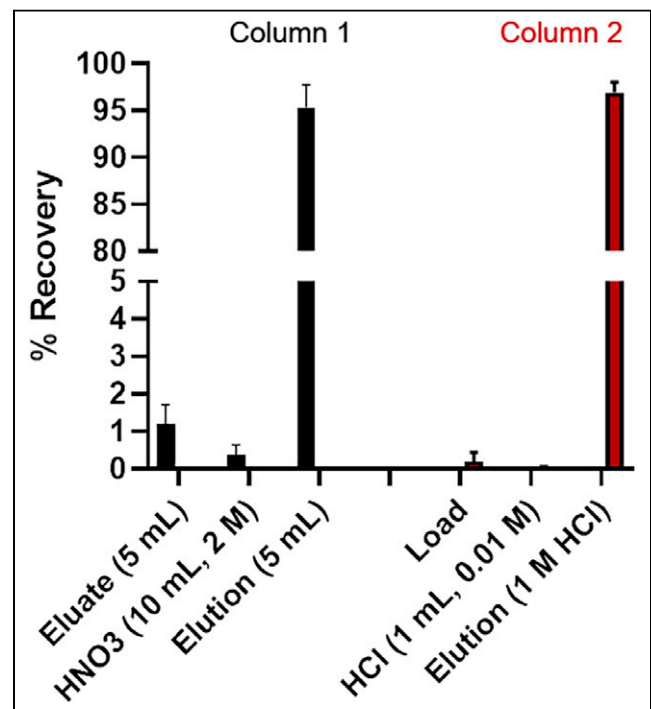


FIGURE 4. Separation results for column 1 and column 2, with percentage recovery of ^{203}Pb ($n = 3$, enriched target material ^{205}Tl).

TABLE 2
ICP-MS Results of Final ^{203}Pb Elution to Determine Metal Contaminants

Backing	Target	Iron	Copper	Zinc	Thallium	Lead
Copper	^{205}Tl	0.01 ± 0.01	0.40 ± 0.48	0.09 ± 0.05	0.22 ± 0.38	0.16 ± 0.06
Gold	^{205}Tl	0.01 ± 0.00	0.01 ± 0.01	0.19 ± 0.08	Below LOD	0.20 ± 0.08

LOD = limit of detection.
Data are micrograms for final elution fraction of 400 μL .

(550 ± 950 ppb or 0.2 ± 0.4 μg) and lead (400 ± 150 ppb or 0.2 ± 0.1 μg) in the final 400 μL elution fraction. Significant SDs were observed in the reported results and are likely due to process variabilities in different batches.

During optimization of the separation method for ^{203}Pb , practical steps were taken to minimize the amount of residual trace metal contaminants in the product solution to improve the overall molar activity. For example, stable lead contamination is one of the primary concerns due to abundance of lead bricks in radiochemistry facilities. Therefore, the working station lead bricks were covered to reduce the amount of nonradioactive lead in the final elution and significantly reduced this contaminant. For copper backings, we found milligram amounts of copper in the dissolved target coming from dissolution of the backing in the HNO_3 , whereas switching to a gold target material alleviated this issue as indicated in Supplemental Table 2. The extraction resin is highly selective for lead isotopes in 2 M HNO_3 , which was confirmed during the separation because minimum breakthrough of lead (<2%) was observed in the flowthrough and the first wash of nitric acid as shown in Supplemental Table 3.

The molar activity of the final elution was also calculated using ICP-MS, and the average specific activity was about 5 $\text{TBq}/\mu\text{mol}$ ($4,745 \pm 2,657$ TBq/g) for an average batch size of 7.5 ± 1.4 GBq/mL (202.5 ± 38.7 mCi/mL).

AMA Evaluation

To determine the AMA, the DO3A chelator was used for titration analysis. Figure 5B represents the instant thin-layer chromatography graph for radiolabeled DO3A. AMA was calculated using the amount of radiolabeled versus free radioisotope. The average AMA (Fig. 6) was 37.7 ± 5.4 $\text{GBq}/\mu\text{mol}$ (1.1 ± 0.1 $\text{Ci}/\mu\text{mol}$) ($n = 3$).

Radiolabeling Studies

Radiolabeling studies were optimized for the VMT- α -NET targeting conjugate, and a molar activity of 40.6 ± 11 $\text{GBq}/\mu\text{mol}$

(1.1 ± 0.3 $\text{Ci}/\mu\text{mol}$) was achieved, indicating a high molar activity of ^{203}Pb . A representative instant thin-layer chromatography silica gel graph illustrating the radiolabeled [^{203}Pb]Pb-VMT- α -NET is shown in Figure 5C. It was important to understand whether the final product remained stable with similar radiolabeling yields over time. Thus, radiolabeling studies were performed for 2 consecutive days, and no changes in labeling efficiency were observed in the final product.

DISCUSSION

This work represents a method of production and separation of ^{203}Pb using an enriched ^{205}Tl reaction route and electrochemistry for target preparation. Thallium metal has a very low melting point, which was initially a concern during targetry optimization. Electroplating of targets from dissolved Tl_2O_3 was determined to be the preferred route. Targets were manufactured that could withstand irradiation times of up to 4 h and currents of 40 μA when irradiated with a 24-MeV incident beam energy without melting. In addition, the electroplated target enabled irradiation at 24-MeV proton incident energy without any degradation, which was not feasible with a powder target.

Irradiated targets resulted in suitable yields with a small amount of target material (<100 mg). However, the plated targets were peeling off when plating density exceeded 150 mg/mm^2 , and no consistent plating results were observed above this density. Therefore, for routine production, the plating density was kept below 150 mg/mm^2 .

The cross section for ^{203}Pb production via the $^{205}\text{Tl}(p,3n)^{203}\text{Pb}$ reaction route is a maximum at 26 MeV ($\sigma = 1,244$ mb), indicating that a 30-MeV cyclotron could produce higher yields. However, a significant amount of the high cross section could be captured with a TR-24 cyclotron. With enriched thallium target material, production yields were significantly higher (32.9 ± 4.1 $\text{MBq}/\mu\text{A-h}$ [0.9 ± 0.1 $\text{mCi}/\mu\text{A-h}$]) than previously published

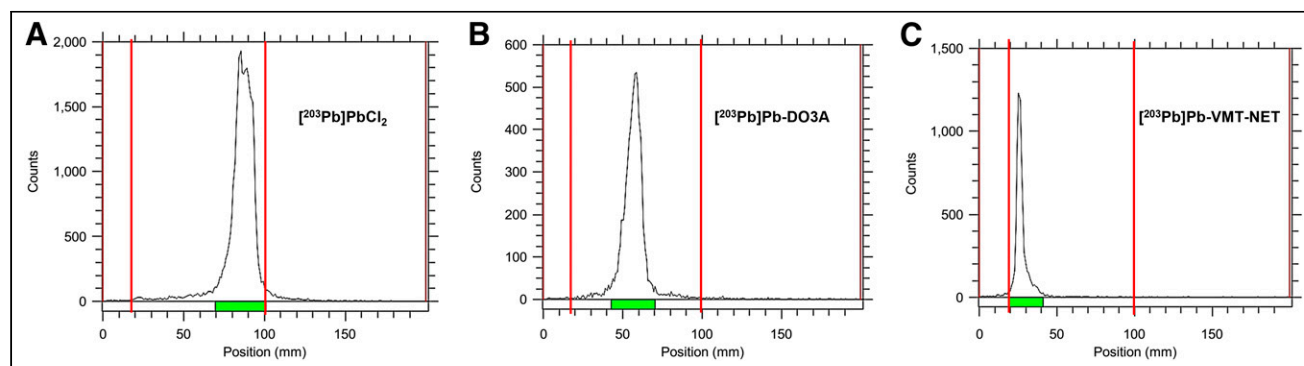


FIGURE 5. Instant thin-layer chromatography silica gel graph for unlabeled [^{203}Pb]PbCl₂ (A), [^{203}Pb]Pb-DO3A (B), and [^{203}Pb]Pb-VMT-NET (C).

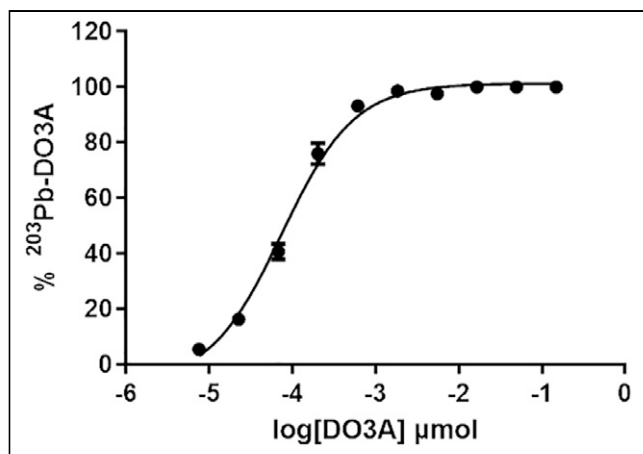


FIGURE 6. Representative AMA measurement for ^{203}Pb Pb-DO3A ($n = 3$).

production routes for $^{203}\text{Tl}(d,2n)^{203}\text{Pb}$ (5.8 MBq/ $\mu\text{A}\cdot\text{h}$ [0.2 mCi/ $\mu\text{A}\cdot\text{h}$]) (17) and $^{203}\text{Tl}(p,n)^{203}\text{Pb}$ (6.3 MBq/ $\mu\text{A}\cdot\text{h}$ [0.2 mCi/ $\mu\text{A}\cdot\text{h}$]) (11). Theoretic production yields were calculated to be 38.1 MBq/ $\mu\text{A}\cdot\text{h}$ (1.03 mCi/ $\mu\text{A}\cdot\text{h}$) for a 100-mg enriched target material with 24-MeV incident beam energy. The experimentally measured results (32.9 ± 4.1 MBq/ $\mu\text{A}\cdot\text{h}$ [0.9 ± 0.1 mCi/ $\mu\text{A}\cdot\text{h}$] [$n = 3$]) were in close agreement with the theoretically predicted numbers for 24-MeV incident proton beam energy.

Isolation and purification of ^{203}Pb from the postirradiation dissolved target using extraction resin chromatography were accomplished using a straightforward method that achieved high recovery yields after separation of more than 95% in the final elution. A small loading volume and controlled flow rate of 0.5 mL/min throughout the separation helped to minimize breakthrough of ^{203}Pb in the loading and washing steps. A second column using weak cation-exchange resin was used to further concentrate and purify ^{203}Pb from any residual Tl or trace metal contaminants and also enabled the final elution in a 400- μL volume. These methods have been tested with up to 3 GBq (80 mCi) of ^{203}Pb , confirming the successful separation. Previous work by Garmestani et al. (17) established separation methods for ^{203}Pb using the $^{203}\text{Tl}(d,2n)^{203}\text{Pb}$ reaction route. However, large elution volumes required additional drying steps resulting in production yields of 2.1 MBq/ $\mu\text{A}\cdot\text{h}$ (0.1 mCi/ $\mu\text{A}\cdot\text{h}$) for natural and 7.5 MBq/ $\mu\text{A}\cdot\text{h}$ (0.2 mCi/ $\mu\text{A}\cdot\text{h}$) for approximately 250-mg enriched ^{203}Tl targets (17). Recent work by McNeil et al. (11) found a successful production method for ^{203}Pb using ^{nat}Tl and ^{203}Tl targets. Although the separation yield was reported to be $73.8\% \pm 2.1\%$, a significant amount of ^{203}Pb was lost in the initial load ($8.7 \pm 0.3\%$) and wash ($\sim 5\%$) steps (11). Recently, Nelson et al. (18) developed a production and separation method using ^{205}Tl as a target material. Their separation method resulted in more than 83% recovery of ^{203}Pb as ^{203}Pb PbCl₂ in a 4-mL final volume in less than 4 h with production yields of 23.3 MBq/ $\mu\text{A}\cdot\text{h}$ (0.6 mCi/ $\mu\text{A}\cdot\text{h}$) using a 250-mg powder target (18). Previous studies reported in the literature also worked with a high amount of starting material—between 250 mg and 4 g (11,18,19). Comparing our results with previous literature, we optimized an electroplating method to produce ^{203}Pb for fast and consistent results with a small amount of starting material (~ 100 mg).

Separation of ^{203}Pb from enriched ^{205}Tl using the extraction resin is very specific to lead, with minimum breakthrough in the initial load and wash (Supplemental Table 3 for complete separation).

The target material was dissolved in HNO₃ (5 mL, 2 M) at a temperature of 90°C and loaded on an extraction resin column. Overall, a very small amount of radioactive waste was generated while keeping the load and wash volumes small.

Gold coins were tested because of high amounts of measured copper (\sim tens of milligrams) in the dissolved target solution when using copper backings. Such high amounts of copper could make it difficult to recycle the enriched target material in the future and introduce a possibility for contamination in the final ^{203}Pb elution. In addition to cold contaminants, the copper backing produces γ -ray emitting zinc isotopes (such as ^{65}Zn ; half-life, 244 d), exposing personnel to potentially higher doses after bombardments. At the current bombardment angle, most of the 24-MeV incident energy is stopped on the copper backing, resulting in long-lived Zn radioisotopes emitting high-energy photons. Comparatively, gold is resistant to dissolution under harsh acid conditions with better heat conductivity. In addition, proton irradiation of gold backing produces mercury isotopes such as $^{197\text{m}}\text{Hg}$ (23.8 h [133 keV (intensity of γ -rays (I_γ), 33.5%), 279 keV (I_γ , 6%)], $^{197\text{g}}\text{Hg}$ (64 h [77 keV (I_γ , 18.7%)]), $^{195\text{m}}\text{Hg}$ (41.6 h [261 keV (I_γ , 31%), 387.8 keV (I_γ , 2.18%), 560 keV (I_γ , 7.1%)]), and $^{195\text{g}}\text{Hg}$ (10.5 h [180 keV (I_γ , 1.9%), 207 keV (I_γ , 1.6%), 261 keV (I_γ , 1.6%), and 585 keV (I_γ , 2%)]). Although these radiocontaminants have a small cross section for energy below 20 MeV, these are relatively short-lived, implying that the gold backing could be reused after a significantly shorter decay time than for a copper backing (the contaminant with the longest half-life is ^{65}Zn : 244 d [1.12 MeV (I_γ , 50%)]), making gold ideal as a backing material.

To compare the difference between electroplated thallium targets using gold and copper backings, high-purity germanium spectra (Supplemental Fig. 2) and ICP-MS analysis (Table 2) results were compared for the dissolved thallium target. ICP-MS analysis from previous studies by McNeil et al. (11) indicated 1.5 ± 0.7 μg of stable lead and 175 ± 105 μg of thallium in the final elution. Higher amounts of trace metal contaminants, specifically stable lead, can affect the molar activity of ^{203}Pb . Our separation resulted in 0.2 ± 0.1 μg of stable lead in a 400- μL final volume, yielding a high molar activity of $4,745 \pm 2,657$ TBq/g (~ 5 TBq/ μmol) ($n = 3$). Previous reports of specific activity range include 52 TBq/g (32 GBq/ μmol) by McNeil et al. (calculated on the basis of the data provided) (11), 405 ± 108 TBq/g by Li et al. (19), and 4,150 TBq/g (2.1 TBq/ μmol) by Nelson et al. (18). Using ICP-MS, molar activity of 266.4 MBq/ μmol (7.2 mCi/ μmol) was reported by Máthé et al. (20) and 15 MBq/ μmol (0.4 mCi/ μmol) by Yao et al. (21), compared with a molar activity of about 5 TBq/ μmol reported in the present study.

The molar activity numbers were not close to the theoretic specific activity of 1.1×10^5 TBq/g (3×10^6 Ci/g), but the numbers reported in this work are the highest yet reported to our knowledge. It is also worth mentioning that the molar activity calculations were performed for small batch sizes of about 3.7 GBq (~ 100 mCi), and we anticipate improvement in these numbers as the batch size increases. AMA was also analyzed using a titration analysis with DO3A chelator, yielding a result of 37.7 ± 5.4 GBq/ μmol (1.1 ± 0.1 Ci/ μmol).

CONCLUSION

This project aimed to develop a robust target preparation method for production of high-specific-activity ^{203}Pb via proton irradiation and an accompanying separation method to address the high demand for ^{203}Pb as an imaging-compatible surrogate for

the in vivo α -particle generator ^{212}Pb . With a suitable half-life (51.8 h), large production batches could be shipped to a large geographic area to fulfill the needs for preclinical and clinical studies. We established a production method using enriched ^{205}Tl and electroplated targets that can withstand beam currents of up to 40 μA . With a 3-h irradiation, an average production yield of 4.6 ± 0.43 GBq (126 ± 11.8 mCi) was obtained. The separation method for ^{203}Pb was developed, and more than 95% overall separation yields were achieved in less than a 400- μL final volume, indicating a robust separation method. A standard operating procedure was also optimized for determining the AMA using DO3A chelator, and a high molar activity of about 37 GBq/ μmol (1 Ci/ μmol) was routinely achieved.

DISCLOSURE

This work was supported by the Department of Energy isotope program through grant DESC0020197 (principal investigator, Suzanne Lapi). This work was also supported in part by Viewpoint Molecular Targeting, now Perspective Therapeutics, of which Nicholas Baumhover and Michael Schultz are employees. No other potential conflict of interest relevant to this article was reported.

KEY POINTS

QUESTION: Is it feasible to produce significant amounts of ^{203}Pb with high molar activity using enriched ^{205}Tl target material?

PERTINENT FINDINGS: An electroplating method was developed to prepare target material (^{205}Tl) that could withstand a 24-MeV incident beam and high current without using a degrader. A separation method was developed to achieve approximately 95% recovery yields of ^{203}Pb with a processing time of less than 1.5 h. ^{203}Pb production batches of 9.2 GBq/mL were achieved using a small amount of target material.

IMPLICATIONS FOR PATIENT CARE: This work addresses a shortage in the availability of the theranostic matched pair $^{203}\text{Pb}/^{212}\text{Pb}$ for clinical applications.

REFERENCES

- Funkhouser J. Reinventing pharma: the theranostic revolution. *Curr Drug Discov*. 2002;2:17–19.
- Gomes Marin JF, Nunes RF, Coutinho AM, et al. Theranostics in nuclear medicine: emerging and re-emerging integrated imaging and therapies in the era of precision oncology. *Radiographics*. 2020;40:1715–1740.
- Elgqvist J, Frost S, Pouget J-P, Albertsson P. The potential and hurdles of targeted alpha therapy: clinical trials and beyond. *Front Oncol*. 2014;3:324.
- FDA approves new diagnostic imaging agent to detect rare neuroendocrine tumors. News release. U.S. Food and Drug Administration; June 1, 2016
- Raedler LA. Lutathera (Lutetium Lu 177 Dotatate) First Radioactive Drug Approved for Gastroenteropancreatic Neuroendocrine Tumors. *J Oncol Navig Surviv*. 2019;9:37–39.
- Fani M, Braun F, Waser B, et al. Unexpected sensitivity of sst2 antagonists to N-terminal radiometal modifications. *J Nucl Med*. 2012;53:1481–1489.
- Fani M, Del Pozzo L, Abiraj K, et al. PET of somatostatin receptor-positive tumors using ^{64}Cu - and ^{68}Ga -somatostatin antagonists: the chelate makes the difference. *J Nucl Med*. 2011;52:1110–1118.
- Horlock P, Thakur M, Watson I. Cyclotron produced lead-203. *Postgrad Med J*. 1975;51:751–754.
- Kratochwil C, Giesel FL, Stefanova M, et al. PSMA-targeted radionuclide therapy of metastatic castration-resistant prostate cancer with ^{177}Lu -labeled PSMA-617. *J Nucl Med*. 2016;57:1170–1176.
- Kratochwil C, Bruchertseifer F, Giesel FL, et al. ^{225}Ac -PSMA-617 for PSMA-targeted α -radiation therapy of metastatic castration-resistant prostate cancer. *J Nucl Med*. 2016;57:1941–1944.
- McNeil BL, Robertson AK, Fu W, et al. Production, purification, and radiolabeling of the $^{203}\text{Pb}/^{212}\text{Pb}$ theranostic pair. *EJNMMI Radiopharm Chem*. 2021;6:6.
- Suparman I. Proposal on “standardized high current solid targets for cyclotron production of diagnostic and therapeutic radionuclides.” In: *Research Co-ordination Meeting of the Co-ordinated Research Project on Standardized High Current Solid Targets for Cyclotron Production of Diagnostic and Therapeutic Radionuclides*. International Atomic Energy Agency; 2000:52–53.
- Queern SL, Aweda TA, Massicano AVF, et al. Production of Zr-89 using sputtered yttrium coin targets. *Nucl Med Biol*. 2017;50:11–16.
- Li M, Baumhover NJ, Liu D, et al. Preclinical evaluation of a lead specific chelator (PSC) conjugated to radiopeptides for ^{203}Pb and ^{212}Pb -based theranostics. *Pharmaceutics*. 2023;15:414.
- Zou Y, Cheng H, Wang H, et al. Thallium (I) oxidation by permanganate and chlorine: kinetics and manganese dioxide catalysis. *Environ Sci Technol*. 2020;54:7205–7216.
- Keith L, Telliard W. ES&T special report: priority pollutants—la perspective view. *Environ Sci Technol*. 1979;13:416–423.
- Garmestani K, Milenic DE, Brady ED, Plascjak PS, Brechbiel MW. Purification of cyclotron-produced ^{203}Pb for labeling Herceptin. *Nucl Med Biol*. 2005;32:301–305.
- Nelson BJ, Wilson J, Schultz MK, Andersson JD, Wuest F. High-yield cyclotron production of ^{203}Pb using a sealed ^{205}Tl solid target. *Nucl Med Biol*. 2023;Jan–Feb:108314.
- Li M, Sagastume EA, Lee D, et al. $^{203}/^{212}\text{Pb}$ theranostic radiopharmaceuticals for image-guided radionuclide therapy for cancer. *Curr Med Chem*. 2020;27:7003–7031.
- Máthé D, Szigeti K, Hegedűs N, et al. Production and in vivo imaging of ^{203}Pb as a surrogate isotope for in vivo ^{212}Pb internal absorbed dose studies. *Appl Radiat Isot*. 2016;114:1–6.
- Yao Z, Garmestani K, Wong KJ, et al. Comparative cellular catabolism and retention of astatine-, bismuth-, and lead-radiolabeled internalizing monoclonal antibody. *J Nucl Med*. 2001;42:1538–1544.
- Yong K, Brechbiel MW. Towards translation of ^{212}Pb as a clinical therapeutic; getting the lead in! *Dalton Trans*. 2011;40:6068–6076.
- Cutler CS, Hennkens HM, Sisay N, Huclier-Markai S, Jurisson SS. Radiometals for combined imaging and therapy. *Chem Rev*. 2013;113:858–883.
- Smith NA, Bowers DL, Eht DA. The production, separation, and use of ^{67}Cu for radioimmunotherapy: a review. *Appl Radiat Isot*. 2012;70:2377–2383.
- Reischl G, Rösch F, Machulla H-J. Electrochemical separation and purification of yttrium-86. *Radiochim Acta*. 2002;90:225–228.
- Geschwind JFH, Salem R, Carr BI, et al. Yttrium-90 microspheres for the treatment of hepatocellular carcinoma. *Gastroenterology*. 2004;127(suppl 1):S194–S205.
- Koehler L, Gagnon K, McQuarrie S, Wuest F. Iodine-124: a promising positron emitter for organic PET chemistry. *Molecules*. 2010;15:2686–2718.
- Kayano D, Kinuya S. Current consensus on I-131 MIBG therapy. *Nucl Med Mol Imaging*. 2018;52:254–265.
- Lehenberger S, Barkhausen C, Cohrs S, et al. The low-energy β^- and electron emitter ^{161}Tb as an alternative to ^{177}Lu for targeted radionuclide therapy. *Nucl Med Biol*. 2011;38:917–924.
- Baum RP, Singh A, Benešová M, et al. Clinical evaluation of the radiolanthanide terbium-152: first-in-human PET/CT with ^{152}Tb -DOTATOC. *Dalton Trans*. 2017;46:14638–14646.
- Carzaniga TS, Auger M, Braccini S, et al. Measurement of ^{43}Sc and ^{44}Sc production cross-section with an 18 MeV medical PET cyclotron. *Appl Radiat Isot*. 2017;129:96–102.
- Rösch F, Baum RP. Generator-based PET radiopharmaceuticals for molecular imaging of tumours: on the way to THERANOSTICS. *Dalton Trans*. 2011;40:6104–6111.
- Singh A, van der Meulen NP, Müller C, et al. First-in-human PET/CT imaging of metastatic neuroendocrine neoplasms with cyclotron-produced ^{44}Sc -DOTATOC: a proof-of-concept study. *Cancer Biother Radiopharm*. 2017;32:124–132.
- Mamtimin M, Harmon F, Starovoitova VN. Sc-47 production from titanium targets using electron linacs. *Appl Radiat Isot*. 2015;102:1–4.
- Domnanich KA, Eichler R, Müller C, et al. Production and separation of ^{43}Sc for radiopharmaceutical purposes. *EJNMMI Radiopharm Chem*. 2017;2:14.